Supporting Information

Cheema et al. 10.1073/pnas.1307935110

SI Materials and Methods

Cell Culture. Mouse 005 glioblastoma stem cells (GSCs) were obtained from I. Verma (Salk Institute, San Diego). These cells are GFP-positive, $p53^{+/-}$, with activated Harvey-Ras^{V12} (Ras) and protein kinase B (Akt) (1). Cultures of 005 GSCs were maintained as spheres in serum-free media, composed of Advanced DMEM/F12 medium (Life Technologies) with L-glutamine (2 mM; Cellgro), 1% N2 supplement (Life Technologies), heparin (2 μg/mL; Sigma), penicillin-streptomycin (Cellgro), recombinant EGF (20 ng/mL; R&D Systems), and recombinant FGF2 (20 ng/mL; Peprotech). Cells were passaged after dissociating neurospheres with TrypLE Express (Life Technologies). Vero cells, obtained from ATCC, were grown in DMEM with 10% (vol/vol) calf serum.

Viruses. Armed G47Δ vectors were constructed using the flip-flop HSV BAC system (2). Mouse IL-12 cDNA (p35 and p40 separated by two bovine elastin motifs) (3) cloned into the shuttle vector plasmid pVec92-fmIL12 was inserted into pG47Δ-BAC using Cre recombinase (New England Biolabs). The BAC sequences were removed by cotransfection with a FLPe recombinase expressing plasmid into Vero cells, and infectious G47Δ-mIL12 (Fig. S2) isolated and plaque purified (4). G47Δ-E (Fig. S2) and G47Δ-mCherry (Fig. S2) were constructed in the same fashion, except with pVec91 and pVec91-mCherry [HSV IE4/5 immediate-early promoter driving mCherry cDNA (provided by Sena Esteves, University of Massachusetts, Worcester, MA)] respectively. G47Δ-Us11fluc was similarly constructed using pFLS-Us11fluc (HSV Us11 late promoter driving firefly luciferase), as described in ref. 5.

Cell Viability Assays. Cells were dissociated and seeded into 96-well plates (4,000 cells per well), treated the next day with either G47Δ-E or G47Δ-mIL12 at the indicated multiplicity of infection (MOI), incubated at 37 °C for up to 96 h, and CellTiter96 AQueous One Solution Cell Viability (MTS) Assays (Promega) performed according to the manufacturer's instructions. Values for virus-infected cells were normalized to those for mock-infected cells (percent cell viability). The experiments were performed in triplicate and repeated at least three times.

Viral Replication Assays. Dissociated GSCs were plated at 8×10^4 cells/250 μL in 24-well plates, incubated overnight at 37 °C, and oncolytic HSV (oHSV) was added to the media at a MOI = 0.1. After 1.5 h for virus adsorption, 250 μL per well of media was added, cells were incubated at 37 °C, and harvested with supernatant at indicated time points. After three freeze–thaw cycles and sonication, the titers of infectious virus were determined by plaque assay on Vero cells.

In Vivo Studies. Immunocompetent C57BL/6 (aged 7–9 wk) and athymic mice were obtained from National Cancer Institute, Frederick, MD. All mouse procedures were approved by the subcommittee on research animal care at Massachusetts General Hospital. Dissociated 005 GSCs ($2–5 \times 10^4$ cells) in 3 μL PBS were implanted stereotaxically into the striatum (2.5-mm lateral from Bregma and 3-mm deep) to generate orthotopic intracranial tumors. On days 8 and 12 after tumor implantation, mice were randomly divided into three groups and intratumorally injected (same stereotaxic coordinates) with G47Δ-E or G47Δ-mIL12 ($\sim 5 \times 10^5$ pfu/3 μL) or PBS. Mice were then followed for signs of discomfort or neurological symptoms and euthanized before becoming moribund (survival, $n = 10$ mice per group).

For quantitative analysis, mice were intratumorally injected with PBS, G47Δ-E, or G47Δ-mIL12 on days 19 and 23 after 005 GSC implantation and then killed 1 and 6 d posttreatment (days 24 and 29). Brain tumor quadrants were excised, minced, and incubated with Accutase (Innovative Cell Technologies) and 10 units/mL DNase I for 10 min at 37 °C, triturated, and passed through a 40-μm cell screen, washed, and resuspended in FACS buffer (PBS + 2 mmol/L of EDTA + 0.5% BSA). Spleens and cervical lymph nodes were harvested, minced, and pushed through 70-μm cell screens to create single cell suspensions. Blood lysis was done as needed with mouse RBC lysis buffer (Boston Bioproducts). Excised brain tumor quadrants were homogenized in PBS for ELISA or with RIPA buffer containing a mixture of protease and phosphatase inhibitors (Boston Bioproducts) for protein lysates.

For bioluminescent imaging (BLI) of virus replication, 1×10^5 005 GSCs were intracerebrally implanted in SCID mice and 13 d later G47Δ-Us11fluc (1×10^6 pfu in 2 μL) was injected into the tumor. At 24, 48, 72, and 144 h postvirus injection mice were anesthesized with 2% isofluorane and BLI was performed after i.p. injection of 4.5 mg D-luciferin (Gold Biotech). Under imaging conditions used (binning, 16 s and exposure, 60 s), the background was below 100 photons/s.

Self-Renewal Neurosphere Formation Assay. Three days after second virus infection, brain tumor quadrants were harvested and sorted for GFP^+ cells by FacsAria. Viable cell (trypan blue excluding) counts were determined, cells resuspended in serum-free media, and seeded into 96-well plates at 10 or 30 cells per well. Fifteen days later, the number of neurospheres (diameter, >60 μm) and wells containing neurospheres were counted. Six mice per group and counts were performed in a blinded manner.

In Vivo NK-Cell Depletion. Mice were intraperitoneally injected with 200 μg anti-NK1.1 antibody (BioXcell) on days 6, 8, and thereafter every 3 d after tumor implantation. NK-cell depletion was confirmed by staining with antibodies to NK1.1 (BD Biosciences), Dx5 (Biolegend), and NKp46 (BD Biosciences), and FACS analysis.

ELISA and Western Blots. Mouse IL-12 and IFN-γ were quantified from cell culture (infected at MOI = 0.1) or brain supernatants using the Quantikine IL-12 and IFN-γ ELISA kits (R&D Systems) as per manufacturer's instructions. Protein concentration in lysates was measured by Bradford assay, and 40 μg of protein loaded onto Precast 4–15% gels (Bio-Rad), electrophoresed, protein transferred to PVDF membranes, and probed with primary antibody against VEGF (Santa Cruz; 1:1,000), IFN-inducible protein 10 (IP-10) (Abcam; 1:2,500), or Actin (1:10,000; Sigma) overnight at 4 °C. This was followed by incubation with appropriate HRP-conjugated goat anti-rabbit (1:5,000; Promega) or anti-mouse (1:10,000; Promega) antibodies for 1 h at room temperature. Protein–antibody complexes were visualized using enhanced chemiluminescence (ECL, Amersham Bioscience). Experiments were performed with three mice per group.

Immunohistochemistry. For histological studies, animals were perfused with 4% paraformaldehyde, brains removed, saturated with 30% sucrose, embedded in Tissue-Tek optimal cutting temperature (OCT), frozen, and sectioned. Eight-micrometer sections were subjected to hematoxylin and eosin staining or immunocytochemistry with antibody against mouse CD31 (BD Pharmingen), VEGF (AbD Serotec), GFAP (Sigma), oligodendrocyte lineage transcription factor 2 (Olig2) (Abcam), or Nestin (Millipore) followed by incubation with appropriate secondary

antibodies (Jackson ImmunoResearch). Microvessel density ($CD31^+$ pixels as a percentage of total pixels from five random fields, $n = 3$ mice per group) was assessed using National Institutes of Health Image J. For immunocytochemistry, neurospheres were plated on coverslips coated with fibronectin overnight, fixed with 4% paraformaldehyde, permeabilized with 0.05% Triton, followed by primary antibodies against Nestin, βIII-tubulin (Millipore), GFAP (Sigma), appropriate fluorescently conjugated secondary antibodies, and DAPI.

Immune Cell Isolation and Flow Cytometry. Fluorescently conjugated antibodies to mouse MHC class I molecules H2- Kb and -Db, MHC class II, CD40, CD86, CD80, CD3e (145-2C11), CD4 (L3T4), CD25 (PC61), forkhead box P3 (Foxp3, FJK-16s), CD45, as well as appropriate isotype controls, were obtained from BD Biosciences, and to CD155 and retinoic acid early inducible-1 [Rae-1 (pan-specific)] from R&D Systems, and to mProminen-1 (mCD133 homolog) from Miltenyi Biotec. Cells were spun, counted, and resuspended in FACS buffer, and incubated with antibodies against surface markers for 30 min at 4 °C in the dark. For intracellular Foxp3 staining, cells were then fixed and permeabilized using 1×Fix/Perm solution (eBioscience), washed in 1× permeabilization buffer (eBioscience), and stained with antibody for 30 min at 4 °C in the dark. Cells were then washed, resuspended in 1× PBS + 2% FCS + 1% buffered neutral formalin, and analyzed on a LSRII flow cytometer (BD Biosciences). Data were analyzed with BD FlowJo software (Tree Star).

Statistical Analysis. Comparisons of data in cell survival and virus yield assays were performed using a two-tailed Student *t* test. Survival data were analyzed by Kaplan Meier survival curves, and comparisons determined by log rank test. *P* values of less than 0.05 were considered significant. Statistical analysis was conducted using Prism software.

1. Marumoto T, et al. (2009) Development of a novel mouse glioma model using lentiviral vectors. *Nat Med* 15(1):110–116.
2. Kuroda T, Martuza RL, Todo T, Rabkin SD (2006) Flip-Flop HSV-BAC: Bacterial artificial chromosome based system for rapid generation of recombinant herpes simplex virus vectors using two independent site-specific recombinases. *BMC Biotechnol* 6:40.
3. Wong RJ, et al. (2001) Cytokine gene transfer enhances herpes oncolytic therapy in murine squamous cell carcinoma. *Hum Gene Ther* 12(3):253–265.
4. Liu TC, et al. (2006) Dominant-negative fibroblast growth factor receptor expression enhances antitumoral potency of oncolytic herpes simplex virus in neural tumors. *Clin Cancer Res* 12(22):6791–6799.
5. Sgubin D, Wakimoto H, Kanai R, Rabkin SD, Martuza RL (2012) Oncolytic herpes simplex virus counteracts the hypoxia-induced modulation of glioblastoma stem-like cells. *Stem Cells Transl Med* 1(4):322–332.
6. Todo T, Martuza RL, Rabkin SD, Johnson PA (2001) Oncolytic herpes simplex virus vector with enhanced MHC class I presentation and tumor cell killing. *Proc Natl Acad Sci USA* 98(11):6396–6401.

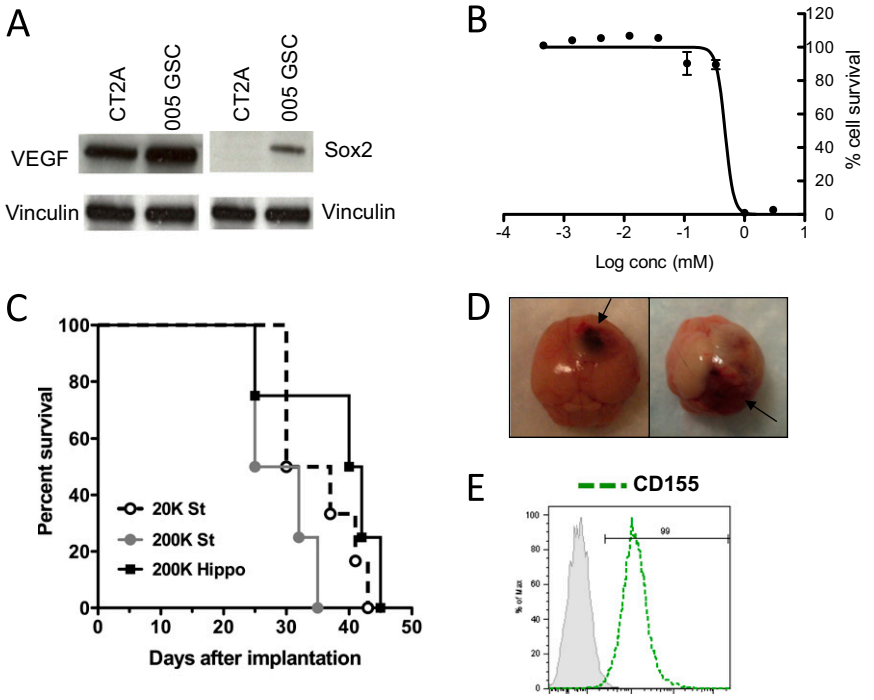

Fig. S1. (*A*) Western blot of SRY-box containing gene 2 (Sox2) and VEGF protein from 005 GSCs and CT2A mouse glioma cell line, both syngeneic to C57BL/6 mice. (*B*) The sensitivity of 005 GSCs to temozolomide was examined after 4 d using an MTS assay. The EC_{50} was ~300 μM. (*C*) 005 GSCs were implanted intracranially in the striatum (St; $2 \times 10^{4 \text{ and } 5}$ cells) and hippocampus (Hippo; 2×10^5 cells) (1.5-mm lateral and 2-mm posterior from Bregma and 2.3-mm deep) of C57BL/6 mice. Glioblastoma (GBM) tumors formed in both locations with a median survival of 26 and 31 d in St and 40 d in Hippo. (*D*) Brains from mice with tumors in St (*Left*) and Hippo (*Right*), note hemorrhage (arrows). (*E*) Expression of CD155 on 005 GSCs by FACS.

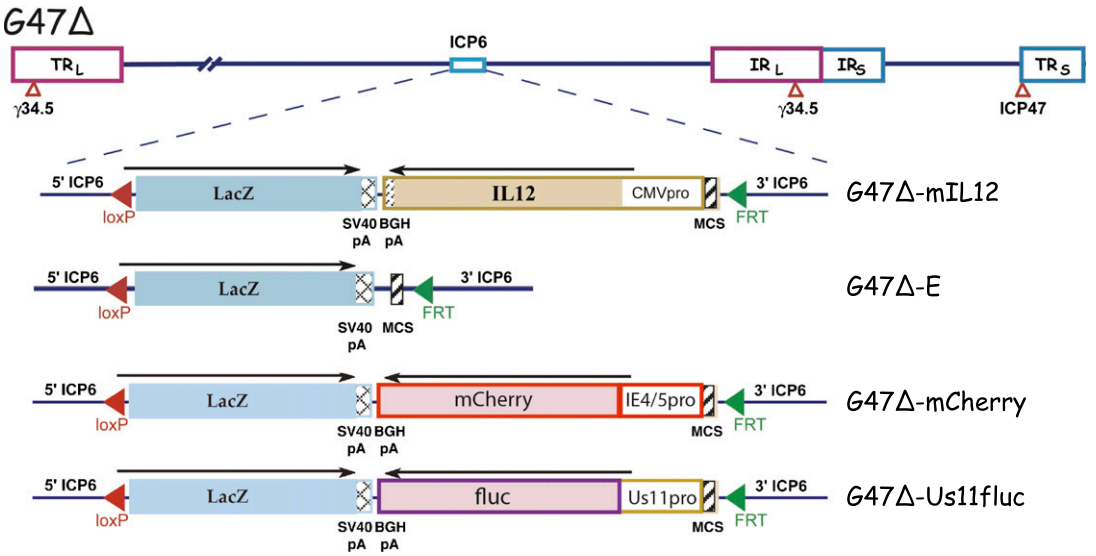

Fig. S2. Construction G47Δ-mIL12. Murine IL-12 was inserted into the backbone of G47Δ using the flip-flop HSV-BAC system (2). G47Δ is a third-generation oHSV with deletions in the γ34.5 and α47 genes and an inactivating LacZ insertion into infected cell protein 6 (ICP6) (6). G47Δ-mIL12 contains an IL-12 fusion protein driven by the CMV immediate-early (IE) promoter. G47Δ-E was constructed at the same time using a shuttle plasmid lacking a transgene. G47Δ-mCherry is similar to G47Δ-mIL12 except the transgene is mCherry, which is driven by HSV-1 IE4/5 promoter. G47Δ-Us11fluc contains firefly luciferase driven by the HSV-1 Us11 late promoter.

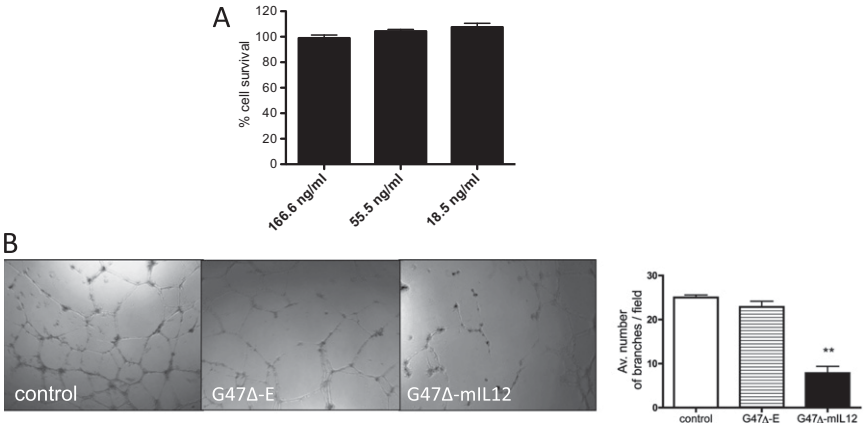

Fig. S3. (*A*) Recombinant IL-12 had no cytotoxic effect on 005 mGSCs over a 4-d period (MTS assay). (*B*) Matrigel-based tube formation of human umbilical vein endothelial cells (HUVECs). HUVECs (Lonza) were grown in endothelial cell growth media (EGM)-2 media supplemented with the bullet kit (Lonza) and maintained in culture for no more than 10 passages. 005 GSCs were infected with oHSV at MOI = 0.8, incubated in EGM-2 media for 24 h and media supernatants collected followed by addition of 1% pooled human gamma globulin (GamaSTAN; Grifols Therapeutics) to neutralize infectious virus. HUVECs (8×10^4 cells) were resuspended in the conditioned media, plated into 24-well plates coated with 250 μL of Matrigel (BD Bioscience) for 20–24 h at 37 °C, and tube formation quantified (counting branches in five random fields per well) and imaged at 20× . Experiment was performed in triplicate. Images of representative wells (*Left*). $^{**}P < 0.01$ (*Right*).

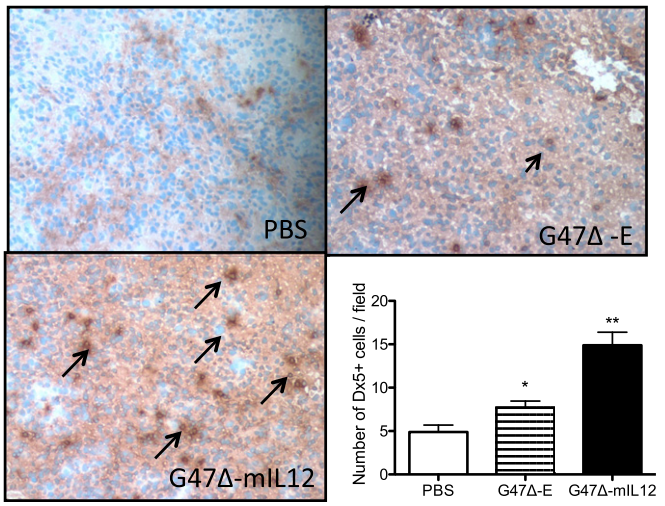

Fig. S4. Immunohistochemical staining of brain tumor sections for NK cells, using anti–NK-CD49d (DX5 clone, 1:100; BioLegend), followed by HR-conjugated secondary antibodies (Vector), and DAB straining (Dako) (arrows) on day 6 posttreatment with PBS, G47Δ-E, or G47Δ-mIL12. Histogram of DX5$^+$ cell counts from five random fields, $n = 2$ per group. G47Δ-E had a slight increase in DX5$^+$ cells over PBS ($^*P < 0.05$), whereas G47Δ-mIL12 treatment significantly increased the number of DX5$^+$ cells over G47Δ-E ($^{**}P < 0.01$).

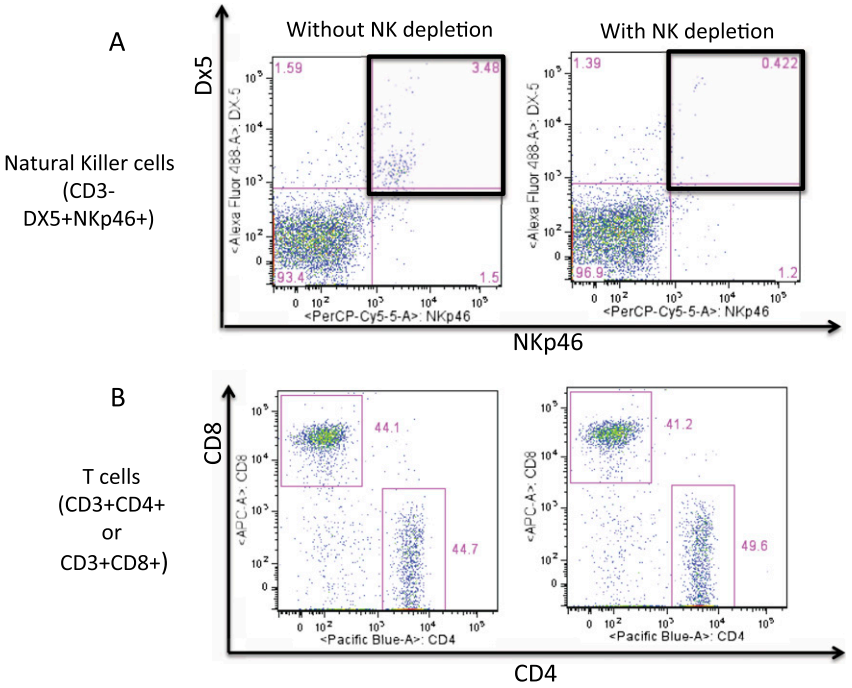

Fig. S5. Spleens from mice treated with (*Right*) or without NK-cell (*Left*) depletion were processed and (*A*) stained with anti-NK cell antibodies (Dx5 and NKp46) to ensure depletion. A significant decrease in NK cells (DX5$^+$NKp46$^+$) was observed, as shown by the representative flow cytometry graphs (black bordered quadrants). (*B*) Staining with anti–T-cell antibodies (CD3, CD4, and CD8). No differences were observed in CD4$^+$ or CD8$^+$ cells (expressed as a percentage of CD3$^+$ cells) in spleens from mice treated either with (*Right*) or without anti–NK-cell antibody (*Left*).

Table S1. T-cell populations in the brain tumor, spleen, and cervical lymph nodes at 6 d posttreatment, expressed as an average percentage from three animals per group ± SEM

Brain tumor	PBS	G47Δ-E	G47Δ-mIL12
$CD3^+$	2.8 ± 0.45	4.4 ± 0.81	3.5 ± 0.4
$CD4^+$ (% of CD3)	22.03 ± 1.4	26.4 ± 1.94	31.5 ± 3.37
$CD8^+$ (% of CD3)	18.77 ± 0.77	19.67 ± 1.65	16.33 ± 1.97
$CD4^+/CD8^+$	1.17 ± 0.05	1.34 ± 0.11	1.93 ± 0.4
$CD4^+CD69^+$	70.6 ± 0.75	71.5 ± 2.57	68.5 ± 2.75
$CD8^+CD69^+$	45.3 ± 3.78	48.3 ± 5.8	41 ± 4.8
Spleen			
$CD3^+$	33.1 ± 1.1	34.4 ± 0.4	34.7 ± 0.9
$CD4^+$ (% of CD3)	44.8 ± 0.6	45.1 ± 0.8	42.9 ± 1.2
$CD8^+$ (% of CD3)	36.3 ± 0.5	37.2 ± 0.9	38.3 ± 0.6
$CD4^+/CD8^+$	1.2 ± 0.03	1.2 ± 0.05	1.1 ± 0.04
$CD4^+CD69^+$	12.6 ± 0.2	15.2 ± 0.7	15.6 ± 1.4
$CD8^+CD69^+$	19.1 ± 1.0	19.4 ± 1.1	15.6 ± 1.4
Cervical lymph nodes			
$CD3^+$	53 ± 2.74	51.8 ± 1.3	46.9 ± 1.5
$CD4^+$ (% of CD3)	48.4 ± 1.8	46.1 ± 1.2	43.7 ± 1.8
$CD8^+$ (% of CD3)	41.4 ± 1.3	40.9 ± 0.7	42.3 ± 0.8
$CD4^+/CD8^+$	1.2 ± 0.08	1.1 ± 0.04	1.05 ± 0.06
$CD4^+CD69^+$	23.1 ± 1.8	25.1 ± 1.3	24.2 ± 1.5
$CD8^+CD69^+$	15.7 ± 2.8	17.9 ± 2.2	15.5 ± 0.9